

# UC Irvine

## UC Irvine Previously Published Works

### Title

Focused ultrasound-mediated sonochemical internalization: an alternative to light-based therapies

### Permalink

<https://escholarship.org/uc/item/89j4n53d>

### Journal

Journal of Biomedical Optics, 21(7)

### ISSN

1083-3668

### Authors

Gonzales, Jonathan  
Nair, Rohit Kumar  
Madsen, Steen J  
[et al.](#)

### Publication Date

2016-07-21

### DOI

10.1117/1.jbo.21.7.078002

Peer reviewed

# Journal of Biomedical Optics

BiomedicalOptics.SPIEDigitalLibrary.org

## **Focused ultrasound-mediated sonochemical internalization: an alternative to light-based therapies**

Jonathan Gonzales  
Rohit Kumar Nair  
Steen J. Madsen  
Tatiana Krasieva  
Henry Hirschberg

**SPIE.**

Jonathan Gonzales, Rohit Kumar Nair, Steen J. Madsen, Tatiana Krasieva, Henry Hirschberg, "Focused ultrasound-mediated sonochemical internalization: an alternative to light-based therapies," *J. Biomed. Opt.* **21**(7), 078002 (2016), doi: 10.1117/1.JBO.21.7.078002.

# Focused ultrasound-mediated sonochemical internalization: an alternative to light-based therapies

Jonathan Gonzales,<sup>a,†</sup> Rohit Kumar Nair,<sup>a,†</sup> Steen J. Madsen,<sup>b</sup> Tatiana Krasieva,<sup>a</sup> and Henry Hirschberg<sup>a,b,\*</sup>

<sup>a</sup>University of California, Beckman Laser Institute, 1002 Health Sciences Road, Irvine, California 92612, United States

<sup>b</sup>University of Nevada, Department of Health Physics, 4505 South Maryland Parkway, Box 453037, Las Vegas, Nevada 89154, United States

**Abstract.** Activation of sonosensitizers via focused ultrasound (FUS), i.e., sonodynamic therapy has been proposed as an extension to light-activated photodynamic therapy for the treatment of brain as well as other tumors. The use of FUS, as opposed to light, allows treatment to tumor sites buried deep within tissues as well as through the intact skull. We have examined ultrasonic activation of sonosensitizers together with the anticancer agent bleomycin (BLM), i.e., sonochemical internalization (SCI). SCI is a technique that utilizes FUS for the enhanced delivery of endo-lysosomal trapped macromolecules into the cell cytoplasm in a similar manner to light-based photochemical internalization. The released agent can, therefore, exert its full biological activity, in contrast to being degraded by lysosomal hydrolases. Our results indicate that, compared to drug or FUS treatment alone, FUS activation of the sonosensitizer AIPcS<sub>2a</sub> together with BLM significantly inhibits the ability of treated glioma cells to grow as three-dimensional tumor spheroids *in vitro*. © 2016 Society of Photo-Optical Instrumentation Engineers (SPIE) [DOI: 10.1117/1.JBO.21.7.078002]

Keywords: chemotherapy; bleomycin; photochemical internalization; sonochemical internalization; glioma therapy; endosomal escape.

Paper 160246R received Apr. 14, 2016; accepted for publication Jul. 7, 2016; published online Jul. 21, 2016.

## 1 Introduction

Although chemotherapy has made great strides in cancer treatment, serious side effects due to toxicity toward normal tissue leads to drug dosages that are often inadequate for complete tumor regression. One of the main limitations to the efficacy of chemotherapy is the inability of drugs to gain entry into cancer cells through the plasma membrane. This barrier limits chemotherapeutic agents to mostly lipophilic or low molecular weight compounds that passively diffuse into the cell cytoplasm. In contrast, many highly effective chemotherapeutic agents are large and water soluble and are actively transported into cells by endocytosis. Their poor ability to escape from the resulting intracellular endosomes leads to their inactivation via lysosome–endosome fusion by the powerful enzyme systems within the lysosome. Therefore, a method that leads to endosomal escape would significantly increase the effect of these agents.

Photochemical internalization (PCI) is a technology that can enhance the delivery of macromolecules in a site-specific manner.<sup>1–5</sup> The concept is based on the use of specially designed photosensitizers, which localize preferentially in the membranes of endosomes. Upon light activation, the photosensitizer interacts with ambient oxygen causing vesicular membrane damage resulting in the release of encapsulated macromolecules into the cell cytosol instead of being transported and degraded in the lysosomes. Initial PCI protocols employed the so-called “light after” approach since it was thought that the photosensitizer and the compound to be released from the endocytic vesicles had to be located in the same compartments at the

time of light exposure.<sup>1,3,6</sup> However, subsequent studies have shown that light can be delivered many hours prior to the delivery of the compound without reducing the efficacy of the combined treatment.<sup>7,8</sup>

An intrinsic drawback of light-based therapies, such as photodynamic therapy (PDT) or PCI, is the limited penetration depth of light in biological tissues. A potential solution is the use of focused ultrasound (FUS) to activate sonosensitizers. FUS activation of sonosensitizers, i.e., sonodynamic therapy (SDT) has been proposed as an alternative to light-activated PDT for the treatment of cancerous tumors including gliomas.<sup>9–15</sup> The use of FUS to activate sonosensitizers would allow treatment to tumor sites buried deep within tissues and through the intact human skull.

We have recently reported a study comparing the increased efficacy of the anticancer drug bleomycin (BLM) activated by FUS or visible light in the presence of sensitizing agents.<sup>16</sup> An *In vitro* model, employing rat glioma monolayer cultures and clonogenicity assays were used. The purpose of the study reported here was to extend the sonochemical internalization (SCI) results found in simple monolayer cultures to a more complex tumor model. *In vitro* models employing multicell glioma spheroids (MGS) were used to ascertain the ability of BLM SCI to inhibit tumor growth. Tumor-cell spheroids are three-dimensional (3-D) aggregates of cells that mimic microtumors and metastases. In comparison to monolayer cultures, a significant advantage of multicell spheroids is that their microenvironment more closely mimics the *in vivo* situation and, therefore, gene expression and the biological behavior of the cells are similar to that encountered in tumor cells *in situ*.<sup>17–19</sup> The basic concepts of FUS-mediated SCI are illustrated in Fig. 1(a).

\*Address all correspondence to: Henry Hirschberg, E-mail: [hhirschb@uci.edu](mailto:hhirschb@uci.edu)

<sup>†</sup>These authors contributed equally.

## 2 Materials and Methods

### 2.1 Cell Lines

The F98 glioma cell line (American Type Culture Collection, Manassas, Virginia) used in all cell spheroid experiments was originally derived from transformed fetal CD Fisher rat brain cells following exposure to ethyl-nitrosourea on the 20th day of gestation.<sup>20,21</sup> The cells were cultured in Dulbecco's Modified Eagle Media (DMEM, Gibco, Carlsbad, California) with high glucose and supplemented with 2-mM L-glutamine, gentamycin (100 mg/ml), and 2% heat-inactivated fetal bovine serum (Gibco) at 37°C in a 7.5% CO<sub>2</sub> incubator.

### 2.2 Sonosensitizer, Bleomycin

Aluminum phthalocyanine disulfonate (AIPcS<sub>2a</sub>; Frontier Scientific, Inc, Logan, Utah), a membrane localizing amphiphilic photosensitizer, proven effective for PCI, was used in all experiments. BLM was obtained from Sigma chemicals (Sigma, St. Louis, Missouri) and diluted in DMEM before use.

### 2.3 Spheroids

#### 2.3.1 Spheroid generation

MGS were formed by a modification of the centrifugation method as previously described.<sup>4,22</sup> Briefly,  $2.5 \times 10^3$  cells in 200  $\mu$ l of culture medium per well were allocated into the wells of ultra-low attachment surface 96-well round-bottomed plates (Corning Inc., New York). The plates were centrifuged at 1000 g for 30 min. Immediately following centrifugation, the tumor cells formed into a disk shape. The plates were maintained at 37°C in a 5% CO<sub>2</sub> incubator for 48 h to allow them to take on the usual 3-D spheroid form. The initial diameter of the spheroids at this point was between 250 and 300  $\mu$ m.

#### 2.3.2 Sonodynamic therapy spheroid toxicity

Forty-eight hours after generation, spheroids were transferred from the microplate wells into 35-mm Petri dishes, 16 to 24 per dish. For SDT evaluation, the spheroids were incubated in 1- $\mu$ g/ml AIPcS<sub>2a</sub> and DMEM for 18 h. Following incubation,

the spheroids were washed three times and allowed a 4-h soak to allow some of the sonosensitizer to leach from the cell membrane. FUS irradiation was performed with a portable FUS generator (SonoCare Plus, Roscoe Medical, Inc. Strongsville, Ohio). The experimental set up is illustrated in Fig. 1(b). The petri dishes containing the spheroids were placed directly on the 3-cm acoustic gel covered FUS transducer head. Sonication was performed at a 100% duty cycle (CW) at a frequency of 1 MHz. FUS exposures ranging from 0 to 0.6 W cm<sup>-2</sup> were examined with a sonication time of 3 min. Control spheroids were sonicated in the absence of sonosensitizers. All sonication procedures were performed at 37 deg and in subdued blue light ambient conditions. Following irradiation, individual spheroids were placed into separate wells of a 96-well culture plate and monitored for growth. Determination of spheroid size was carried out by averaging two measured perpendicular diameters of each spheroid using an inverted microscope with a calibrated measurement scale superimposed in the eyepiece ocular allowing direct evaluation of the spheroid's diameter. Spheroid volume was calculated assuming a perfect sphere. Typically, 16 to 24 spheroids were followed in each trial. Since each trial was performed three times, a total of 48 to 72 spheroids were followed for a given set of parameters. Spheroids were followed for up to 14 days.

#### 2.3.3 Bleomycin toxicity

Forty-eight hours after generation of the F98 spheroids, BLM in a concentration range of 0.3 to 2.4  $\mu$ g/ml was added directly to the wells of the microplate. The spheroids were monitored for growth as previously described, for 14 days. Typically, eight spheroids were followed for each drug concentration in each trial. Identical trials were performed three times. Spheroid growth was followed for 14 days.

#### 2.3.4 Sonochemical internalization spheroid toxicity

Forty-eight hours after generation, spheroids were incubated with 1- $\mu$ g/ml AIPcS<sub>2a</sub> and DMEM for 18 h followed by a triple wash in DMEM. The spheroids were allowed a 4-h soak to allow some of the sonosensitizer to leach from the cell membrane. They were thereafter transferred from the microplate wells

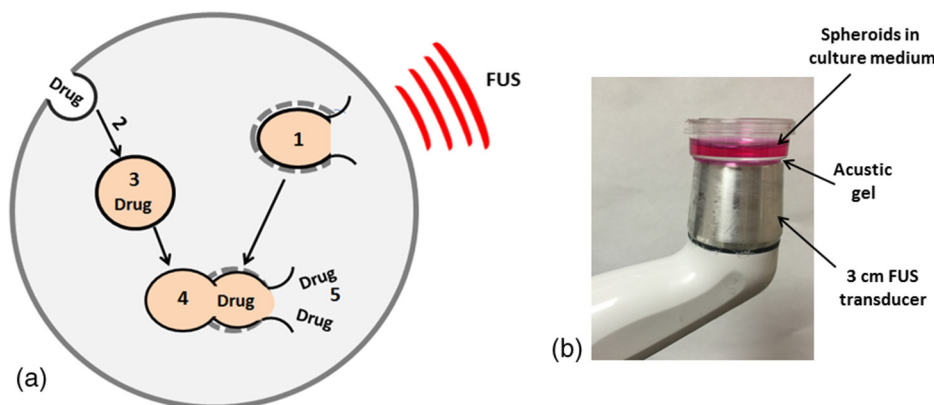


**Fig. 1** (a) "FUS before drug": (1) FUS-induced disruption of endo-lysosome membranes containing photosensitizer before (2) drug is endocytosed and (3) localized in intact endocytic vesicles. (4) Fusion between intact drug-containing and photochemically disrupted photosensitizer containing endosomes leads to (5) the cytosolic release of the drug. (b) Sonication set-up; petri dishes containing multiple spheroids were placed directly on the 3-cm acoustic gel covered FUS transducer head. All sonication procedures were performed at 37 deg and in subdued ambient blue light conditions.

into 35-mm Petri dishes, eight per dish and BLM was added to the cultures (0 to 1  $\mu\text{g}/\text{ml}$ ) to be evaluated for the effects of SCI. A group of the spheroids received BLM but no sonosensitizers (FUS+BLM control) and another group received sonosensitizers but no drug (SDT control). FUS sonication was performed immediately after BLM introduction in an identical manner to that used for the SDT toxicity study. Following sonication, individual spheroids were placed into separate wells of the original 96-well culture plate and monitored for growth as previously described. Typically, eight spheroids were followed in each trial. Since each trial was performed three times, a total of 24 were followed for a given set of parameters. Spheroid growth was followed for 14 days.

### 2.3.5 Live/dead assay

Forty-eight hours after SDT or SCI treatment, two to three spheroids were transferred to glass substrate imaging dishes, stained using a combination of Hoechst 33342 and Ethidium Homodimer 1 (Invitrogen H1399, Carlsbad, California) for 1 h, washed and visualized using a two-photon inverted Zeiss laser-scanning fluorescent microscope (LSM 410, Carl Zeiss, Jena, Germany). This system allows the differential visualization of cell nuclei using confocal and two-photon microscopy. Simultaneously detected blue and red emissions were isolated by using BP 390-465 IR and BP 565-615 IR band pass filters, respectively. Fluorescent images were pseudocolored blue (live) and red (dead).

### 2.4 Endosome Labeling

A number of  $20 \times 10^3$  F98 cells were cultured in glass substrate imaging dishes for 24 h. The cells were then incubated with 1- $\mu\text{g}/\text{ml}$  AIPcS<sub>2a</sub> for 18 h, washed and labeled with LysoTracker Green DND (Thermo Fisher Scientific). LysoTracker probes are fluorescent acido tropic probes for labeling and tracking acidic organelles like endosomes or lysosomes in live cells. The cells were sonicated with an FUS irradiation of 0.2  $\text{W cm}^{-2}$  for 3 min. One hour after FUS sonication, the cells were examined by fluorescent microscopy.

### 2.5 Statistical Analysis

All data were analyzed and graphed using Microsoft Excel. The arithmetic mean and standard error were used in all cases. Statistical significance was calculated using the Student's t-test as well as the Welch's t-test. Two values were considered distinct when their  $p$ -values were below 0.05. Synergism was calculated when analyzing SCI treatments. The following equation was used to determine if the SCI effect was synergistic, antagonistic, or additive:

$$\alpha = \frac{\text{SF}^a \times \text{SF}^b}{\text{SF}^{ab}}$$

In this scheme  $\text{SF}^a$  and  $\text{SF}^b$  represent the survival fraction for SDT and BLM, respectively, and  $\text{SF}^{ab}$  represents the survival fraction for the combined treatment. If two treatments are to be compared, the survival fractions of each separate treatment are multiplied together and then divided by the survival fraction when both treatments are applied together. The resulting number ( $\alpha$ ) describes the cumulative effect. If  $\alpha > 1$ , the result is synergistic. If  $\alpha < 1$ , the result is antagonistic, and if  $\alpha = 1$ , the result is simply additive.

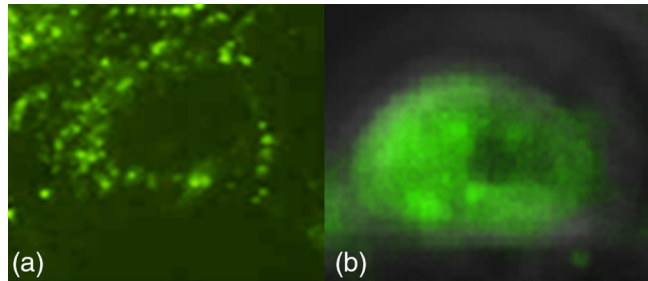


**Fig. 2** FUS-mediated endosomal escape. F98 cells were incubated with 1- $\mu\text{g}/\text{ml}$  AIPcS<sub>2a</sub> for 18 h, washed and labeled with LysoTracker Green DND. (a) Without exposure to FUS. (b) Cells sonicated with 0.2  $\text{W cm}^{-2}$ , and then labeled immediately with LysoTracker for 30 min.

## 3 Results

### 3.1 Endosomal Escape of AIPcS<sub>2a</sub> After Focused Ultrasound Sonication

Fluorescence microscopy was used to verify the uptake and intracellular localization of the LysoTracker probe in the absence or presence of US or light (Fig. 2). The well-defined granules inside endosomes seen before FUS sonication [Fig. 2(a)] change to a much more diffuse distribution throughout the cell after FUS exposure [Fig. 2(b)] demonstrating endosomal escape of the tracker dye.

### 3.2 Effects of Focused Ultrasound, Sonodynamic Therapy, and Bleomycin on F98 Spheroid Growth

To determine the optimal parameters for evaluating the effects of SCI on the F98 spheroids, titrations of drug concentration and FUS exposure were performed. The results are shown in Figs. 3(a) and 3(b) for increasing sonication exposure and drug concentration, respectively.

The data demonstrated the ability of FUS, in the absence of sonosensitizers, to inhibit spheroid growth at higher sonication exposures (0.6  $\text{W cm}^{-2}$ ). A significant increase in the inhibitory effect of FUS can be seen in the presence of sonosensitizers [Fig. 3(a)] compared to FUS alone. The F98 spheroids were also sensitive to BLM exposure. Significant spheroid inhibition was observed at drug concentrations exceeding 0.6  $\mu\text{g}/\text{ml}$  [Fig. 3(b)].

### 3.3 Sonochemical Internalization-Mediated Bleomycin Effects on F98 Spheroid Growth

Originally, the PCI method was shown to be effective for the liberation of drugs that had already been endocytosed and trapped in endocytic vesicles, i.e., it was based on illumination after drug incubation, the so-called “light after” strategy.<sup>1,3,6</sup> In contrast, a number of studies have demonstrated efficacy when photochemical disruption of endocytic vesicles occurs before delivery of macromolecules, i.e., the “light before” strategy.<sup>7,8</sup> These two approaches, FUS before and after drug addition, were examined in our previous study.<sup>16</sup> The results clearly demonstrated that FUS immediately after drug addition was the most efficient protocol and was therefore adopted in these experiments.

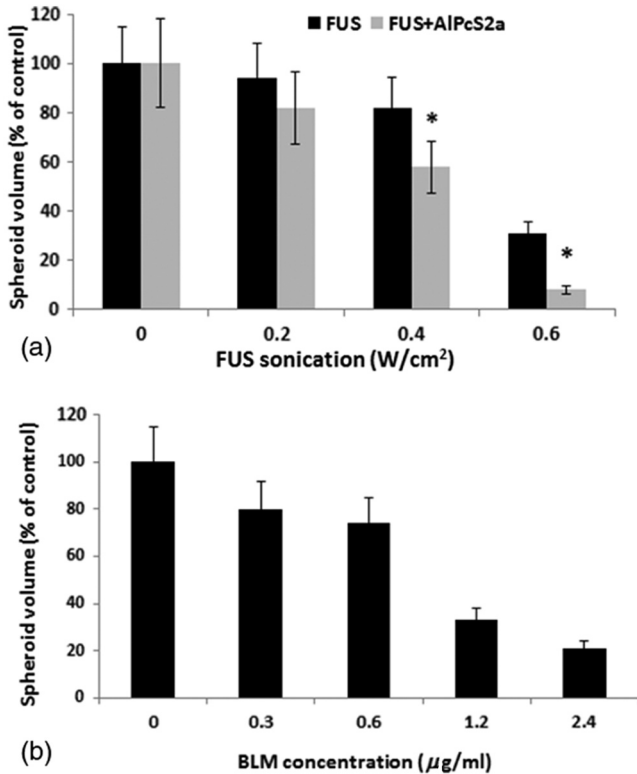


**Fig. 3** Inhibitory effects of SDT and BLM on F98 spheroid growth. (a) Spheroids incubated with 1- $\mu\text{g/ml}$  AIPcS<sub>2a</sub> for 18 h. FUS parameters: frequency of 1 MHz (CW), exposure of 0.2, 0.4, or 0.6  $\text{W cm}^{-2}$ ; exposure time of 3 min. (b) Spheroids incubated with increasing concentrations of BLM. Each data point represents spheroid volume after 2 weeks in culture as a percent of untreated controls and the mean of three experiments. Error bars denote standard errors. Asterisks (\*) denote significant differences ( $p < 0.05$ ) compared to control values.

Experiments were performed on BLM and AIPcS<sub>2a</sub> + BLM + FUS (SCI) treated spheroids using a 3-min 0.2  $\text{W cm}^{-2}$  FUS sonication exposure and 1- $\mu\text{g/ml}$  AIPcS<sub>2a</sub>. Figure 4(a) shows the average spheroid volume as a percent of controls measured after a two week period. BLM concentrations of 0 to 1.2  $\mu\text{g/ml}$  were examined. Three identical experiments were performed with 16 spheroids in each group per experiment. As seen in the figure, FUS in the presence of photosensitizer significantly increased the efficacy BLM at all drug concentrations examined [Fig. 4(a)]. BLM SCI was also compared to the effects of SDT for a sonication range of 0 to 0.6  $\text{W cm}^{-2}$  [Fig. 4(b)]. At FUS sonication exposures of 0.2 or 0.4  $\text{W cm}^{-2}$ , SCI (BLM concentration 0.5  $\mu\text{g/ml}$ ) had a pronounced inhibitory effect on spheroid growth compared to SDT. At high FUS exposure (0.6  $\text{W cm}^{-2}$ ), both SDT and SCI were highly inhibitory, reducing spheroid volume to 18% and 8%, respectively, compared to nontreated controls. The effects of FUS on BLM in the absence and presence of sonosensitizers are compared in Fig. 4(c). Drug efficacy in the absence of sonosensitizer was clearly increased by FUS sonication and was significant ( $p < 0.05$ ) at 0.4  $\text{W cm}^{-2}$ . In contrast though, the addition of sonosensitizer, i.e., SCI, greatly enhanced the potency of BLM compared to FUS+BLM.

Since SCI is a technique that relies on the combination of drug, sonosensitizer, and FUS exposure, the resultant toxicities should show more than an additive effect of the single modalities. The degree of synergism was calculated by comparing the

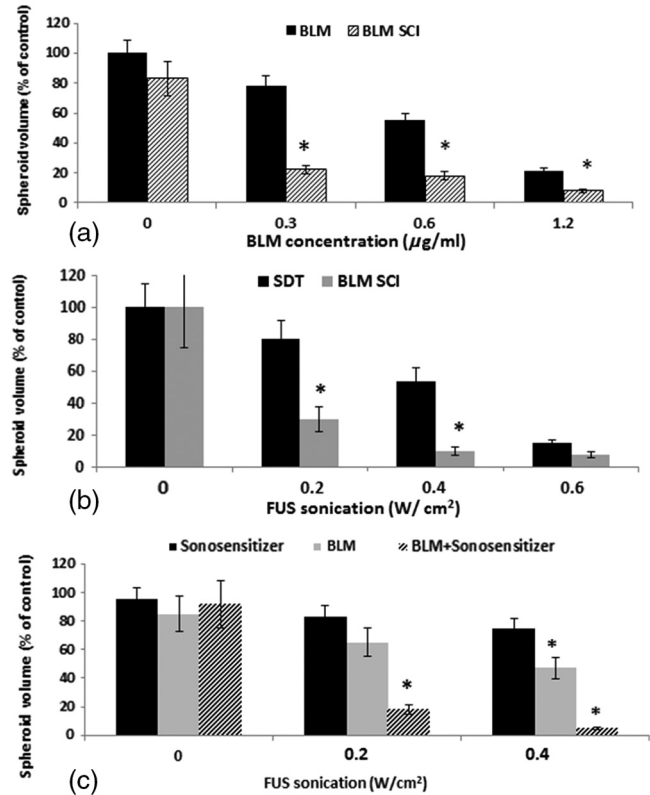


**Fig. 4** SCI growth inhibiting effect. (a) BLM and AIPcS<sub>2a</sub> + BLM + FUS (SCI) treated spheroids using 0.2  $\text{W cm}^{-2}$  FUS sonication exposure for 3 min and 1- $\mu\text{g/ml}$  AIPcS<sub>2a</sub>. (b) SDT and SCI (BLM concentration of 0.5  $\mu\text{g/ml}$ ) in the absence and presence of sonosensitizers, BLM concentration of 0.5  $\mu\text{g/ml}$ . (c) Effects of FUS on BLM efficacy in the absence and presence of sonosensitizers, BLM concentration of 0.5  $\mu\text{g/ml}$ . Each data point represents spheroid volume after 2 weeks in culture as a percent of untreated controls and is the mean of three experiments. Error bars denote standard errors. Asterisks (\*) denote significant differences ( $p < 0.05$ ) compared to control values.

survival fractions of FUS+BLM or SDT alone with that of SCI treatment using the data from Fig. 3(c). As evidenced from the calculated  $\alpha$  values, SCI demonstrated a synergistic effect, especially at the higher FUS sonication levels:  $\alpha = 3.3$  and 5.4 for 0.2 and 0.4  $\text{W cm}^{-2}$ , respectively (the higher the  $\alpha$  value, the greater the degree of synergism). Even in the absence of sonosensitizer, FUS exposure increased the efficacy of BLM (BLM versus BLM+FUS group). Calculated  $\alpha$  values in this case were 0.95 and 1.5 for 0.2 and 0.4  $\text{W cm}^{-2}$  FUS exposures, respectively. This clearly demonstrated a synergistic effect of SCI compared to SDT or FUS+BLM applied independently.

### 3.4 Kinetics of Spheroid Growth

As has been demonstrated previously, inadequate PDT or PCI can induce a growth delay of spheroids, followed by recovery from the effects of treatment, and renewed growth. The growth of F98 spheroids following BLM, SDT, and SCI was therefore examined. Treatment was delivered at an exposure of 0.2  $\text{W cm}^{-2}$  for 3 min and a BLM concentration of 0.5  $\mu\text{g/ml}$ .

As seen from Fig. 5, the SDT treated spheroids were significantly different from nontreated controls at week 1 of incubation but were not significantly different from these controls by week 2. In contrast, SCI-treated cultures, at similar exposures, showed complete inhibition of growth after 7 and 14 days in culture.

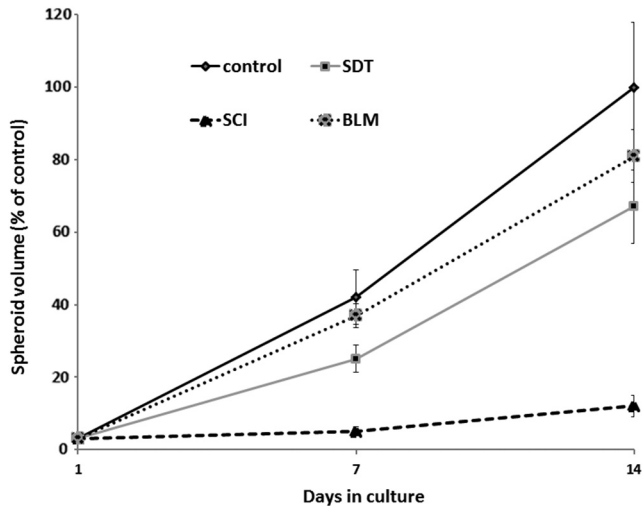


**Fig. 5** Kinetics of spheroid growth following treatment ( $0.2 \text{ W cm}^{-2}$  3 min exposure, BLM concentration of  $0.5 \mu\text{g/ml}$ ). Each data point represents spheroid volume after 2 weeks in culture as a percent of untreated controls and is the mean of three experiments. Error bars denote standard errors. Asterisks (\*) denote significant differences ( $p < 0.05$ ) compared to control values (only three of the four curves are labeled).

### 3.5 Two-Photon Fluorescence Microscopy

The results of live/dead assays employing two-photon fluorescence images demonstrated enhanced toxicity of SCI-treated spheroids compared to BLM or SDT applied as single treatments (Fig. 6). This was inferred from the high proportion of red fluorescing cells observed from the SCI-treated spheroids Fig. 6(d).

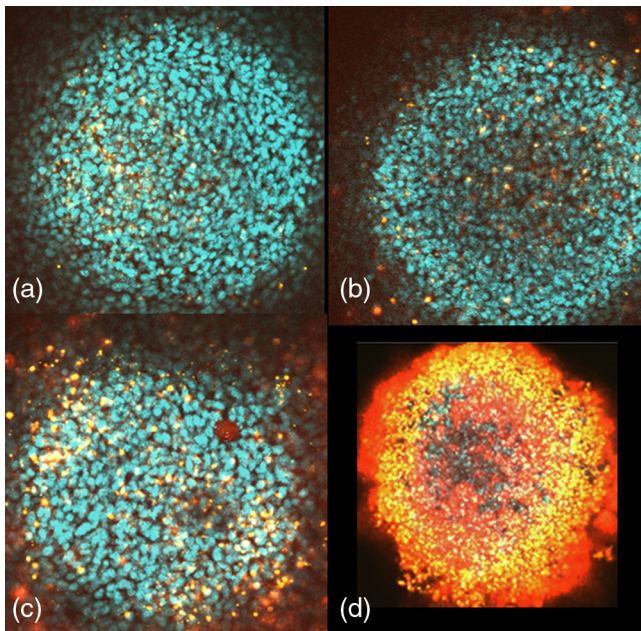


**Fig. 6** Live/dead assay of control and SCI-treated spheroids. Two-photon fluorescence microscopy images of F98 spheroids stained with Hoechst 33342 (blue: live) and Ethidium Homodimer (red: dead). Spheroids were stained 24 h after treatment: (a) control, (b) BLM  $1 \mu\text{g/ml}$  (c) SDT;  $0.2 \text{ W cm}^{-2}$ , 3 min exposure at 1 MHz, (d) SCI;  $1.0 \mu\text{g/ml}$  BLM,  $0.2 \text{ W cm}^{-2}$ , 3 min exposure at 1 MHz. Field of view for all images was  $400 \times 400 \mu\text{m}$ .

By comparison, a smaller number of red fluorescing cells were observed from SDT-only spheroids Fig. 6(c) and these were mainly at the spheroid periphery. As illustrated in Fig. 6, virtually no dead cells were observed in either control Fig. 6(a) or BLM only Fig. 6(b) treated spheroids.

## 4 Discussion

The primary objective of this study was to examine the ability of SCI to synergistically increase the efficacy of BLM chemotherapy on glioma cell tumor spheroids. The results shown in Fig. 4(c) appear to demonstrate that FUS can potentiate the cytotoxic effects of BLM both in the absence and presence of sonosensitizers compared to drug alone. This indicates that two processes are involved. One explanation for the increased efficacy caused by FUS in the absence of sonosensitizers is sonoporation of the cell membrane.<sup>23–25</sup> Although cells are usually exposed to FUS in the presence of microbubbles, ultrasound alone has also been shown to enhance delivery of DNA and drugs.<sup>26,27</sup> In the presence of sonosensitizers, the FUS-mediated-enhanced inhibitory growth effect of BLM is postulated to be due to endosomal escape, in a similar manner to PCI.<sup>3</sup>

FUS SCI-mediated endosomal escape is in all probability caused by the disruption of intracellular endosome membranes containing sonosensitizers. The results shown in Fig. 2 using a LysoTracker probe for labeling endosomes demonstrated that in nontreated cells, the tracker dye localized in granular organelles representing endosomes and lysosomes. In contrast, following FUS exposure, a diffuse fluorescence throughout the cytosol was observed clearly indicating effective escape. These results are in good agreement with those obtained for the effects of light or FUS on photo/sonosensitizer distribution. In previously published experiments, fluorescence microscopy demonstrated the uptake and intracellular localization of the photosensitizer AIPcS<sub>2a</sub> and its redistribution in a similar manner to that shown in Fig. 2 for both PCI and SCI.<sup>16</sup>

The basic mechanism causing both cell plasma and endosome membrane disruption, is thought to be similar for both PCI and SCI, which are based on PDT or SDT effects, respectively. However, there is still some debate as to the exact mechanism of SDT effects on cells.<sup>28–31</sup> It has been postulated that ultrasound inertial cavitation is central to the production of singlet oxygen via sonoluminescence emission. According to this explanation, singlet oxygen generation results from indirect photo-activation of the sensitizing drug. Although the main absorption peak of AIPcS<sub>2a</sub> occurs at  $\sim 670 \text{ nm}$ , a secondary peak (25% of the main peak intensity) can be found at  $350 \text{ nm}$ , which overlaps with the most intense region of the sonoluminescence emission spectrum ( $\sim 200$  to  $400 \text{ nm}$ ), thus providing the possibility of significant singlet oxygen formation.

BLM is a low molecular weight (1.5 kDa) hydrophilic chemotherapeutic agent that is known to accumulate in endocytic vesicles.<sup>32</sup> Its limited ability to escape from endosomes results in its inactivation via hydrolytic enzymes. If released into the cytosol, BLM rapidly diffuses to the nucleus where it has significant toxic effects resulting in single and double strand DNA breaks in a manner similar to the effects observed with ionizing radiation.<sup>33</sup> The observation that a single molecule of BLM is capable of yielding 15 DNA strand breaks makes it the most efficient chemotherapeutic agent. For example, studies using selective electroporation of the plasma membrane have demonstrated a 100-fold increase in BLM toxicity<sup>34</sup> and provide the rationale for the PCI or SCI approach in which

membrane permeabilization is achieved via laser or FUS activation of membrane-bound photo/sono sensitizers. This is in agreement with the findings of other studies in which PCI has been shown to increase the efficacy of BLM in a number of different cell lines.<sup>2,4,5</sup>

SCI of BLM significantly increased its efficacy several fold as is clearly seen in Figs. 4 and 5. The  $\alpha$  values obtained showed a significant degree of synergism of SCI compared to SDT or drug. It is premature to translate the *in vitro* results obtained in this study into results on animal models or clinical expectations. Nevertheless, SCI has the potential to lower both drug concentrations and the number of repetitive doses required to achieve efficacy equal to those obtained with drug alone. The toxic side effects of chemotherapy currently encountered could potentially be reduced significantly.

## 5 Conclusions

SCI is a promising new technology that, like PCI, can potentiate the efficacy of a wide variety of therapeutic compounds. However, unlike PCI, SCI is not limited by the poor tissue penetration inherent to light-based approaches and, as such, this ultrasound-based technology is ideally suited for the treatment of deep seated or intracranial lesions like gliomas.

## Acknowledgments

The authors are grateful for support from the Norwegian Radium Hospital Research Foundation. Portions of this work were made possible through access to the LAMMP Program NIBIB P41EB015890. Steen Madsen acknowledges the support of the Tony and Renee Marlon Charitable Foundation.

## References

1. K. Berg et al., "Photochemical internalization: a novel technology for delivery of macromolecules into cytosol," *Cancer Res.* **59**, 1180–1183 (1999).
2. O. J. Norum et al., "Photochemical internalization of bleomycin is superior to photodynamic therapy due to the therapeutic effect in the tumor periphery," *Photochem. Photobiol.* **85**(3), 740–749 (2009).
3. P. K. Selbo et al., "Photochemical internalization provides time and space-controlled endolysosomal escape of therapeutic molecules," *J. Control Release.* **148**(1), 2–12 (2010).
4. M. S. Mathews et al., "Photochemical internalization of bleomycin for glioma treatment," *J. Biomed. Opt.* **17**(5), 058001 (2012).
5. O. A. Gederaas et al., "Photochemical internalization of bleomycin and temozolomide—in vitro studies on the glioma cell line F98," *Photochem. Photobiol. Sci.* **14**(7), 1357–1366 (2015).
6. M. Brandal Berstad, A. Weyergang, and K. Berg, "Photochemical internalization (PCI) of HER2-targeted toxins Synergy is dependent on the treatment sequence," *Biochim. Biophys. Acta* **1820**, 1849–1858 (2012).
7. L. Prasmickaite et al., "Photochemical disruption of endocytic vesicles before delivery of drugs: a new strategy for cancer therapy," *Br. J. Cancer* **86**, 652–657 (2002).
8. W. Peng et al., "Photochemical internalization (PCI)-mediated enhancement of bleomycin cytotoxicity by liposomal mTHPC formulations in human head and neck cancer cells," *Lasers Surg. Med.* **46**(8), 650–658 (2014).
9. S. Umemura et al., "Mechanism of cell damage by ultrasound in combination with hematoporphyrin," *Jpn. J. Cancer Res.* **81**, 962–966 (1990).
10. M. Nonaka et al., "Sonodynamic therapy consisting of focused ultrasound and photosensitizer causes a selective antitumor effect in a rat intracranial glioma model," *Anticancer Res.* **29**, 943–950 (2009).
11. E. J. Jeong et al., "Sonodynamically induced antitumor effects of 5-aminolevulinic acid and fractionated ultrasound irradiation in an orthotopic rat glioma model," *Ultrasound Med. Biol.* **38**(12), 2143–2150 (2012).
12. D. Costley et al., "Treating cancer with sonodynamic therapy: a review," *Int. J. Hyperthermia* **31**(2), 107–117 (2015).
13. A. P. McHale et al., "Sonodynamic therapy: concept, mechanism and application to cancer treatment," *Adv. Exp. Med. Biol.* **880**, 429–450 (2016).
14. T. Osaki et al., "Sonodynamic therapy using 5-aminolevulinic acid enhances the efficacy of bleomycin," *Ultrasonics* **67**, 76–84 (2016).
15. T. Osaki et al., "Bleomycin enhances the efficacy of sonodynamic therapy using aluminum phthalocyanine disulfonate," *Ultrason. Sonochem.* **28**, 161–168 (2016).
16. S. J. Madsen et al., "Comparing the effects of light or sonic activated drug delivery; photo/sono chemical internalization," *J. Environ. Pathol. Toxicol. Oncol.* **35**(1), 91–98 (2016).
17. R. M. Sutherland, "Cell and environment interactions in tumor micro-regions: the multicell spheroid model," *Science* **240**, 177–184 (1988).
18. M. T. Santini et al., "Apoptosis, cell adhesion and the extracellular matrix in the three-dimensional growth of multicellular tumor spheroids," *Crit. Rev. Oncol. Hematol.* **36**, 75–87 (2000).
19. S. J. Madsen et al., "Multicell tumor spheroids in photodynamic therapy," *Lasers Surg. Med.* **38**(5), 555–564 (2006).
20. R. F. Barth, "Rat brain tumor models in experimental neurooncology: the 9L, C6, T9, F98, RG2 (D74), RT-2 and CNS-1 gliomas," *J. Neurooncol.* **36**(1), 91–102 (1998).
21. S. J. Madsen, K. Kharkhuu, and H. Hirschberg, "Utility of the F98 rat glioma model for photodynamic therapy," *J. Environ. Pathol. Toxicol. Oncol.* **26**(2), 149–155 (2007).
22. A. Ivascu and M. Kubbies, "Rapid generation of single-tumor spheroids for high-throughput cell function and toxicity analysis," *J. Biomol. Screen* **11**(8), 922–932 (2006).
23. S. Bao, B. D. Thrall, and D. L. Miller, "Transfection of a reporter plasmid into cultured cells by sonoporation in vitro," *Ultrasound Med. Biol.* **23**, 953–959 (1997).
24. J. Pepe, M. Rincon, and J. Wu, "Experimental comparison of sonoporation and electro-poration in cell transfection applications," *Acoust. Res. Lett. Online* **5**, 62–67 (2004).
25. A. Yudina, M. Lepetit-coiffé, and C. T. Moonen, "Evaluation of the temporal window following ultrasound-mediated cell membrane permeability enhancement," *Mol. Imaging Biol.* **13**(2), 239–249 (2011).
26. J. Wu, J. Pepe, and M. Rinco, "Sonoporation, anti-cancer drug and antibody delivery using ultrasound," *Ultrasonics* **44**, e21–e25 (2006).
27. V. Frenkel, "Ultrasound mediated delivery of drugs and genes to solid tumors," *Adv. Drug Delivery Rev.* **60**, 1193–1208 (2008).
28. D. Kessel et al., "Porphoryn-induced enhancement of ultrasound toxicity," *Int. J. Radiat. Biol.* **66**, 221–228 (1994).
29. S. J. Putterman and K. R. Weninger, "Sonoluminescence; how bubbles turn sound into light," *Annu. Rev. Fluid Mech.* **32**, 445–476 (2000).
30. N. Miyoshi, T. Igarashi, and P. Riesz, "Evidence against singlet oxygen formation by sonolysis of aqueous oxygen-saturated solutions of hematoporphyrin and Rose Bengal the mechanism of sonodynamic therapy," *Ultrason. Sonochem.* **7**, 121–124 (2000).
31. M. W. Miller, D. L. Miller, and A. A. Brayman, "A review of in vitro bioeffects of inertial ultrasonic cavitation from a mechanistic perspective," *Ultrasound Med. Biol.* **22**, 1131–1154 (1996).
32. G. Pron et al., "Internalization of the bleomycin molecules responsible for bleomycin toxicity: a receptor-mediated endocytosis mechanism," *Biochem. Pharmacol.* **57**(1), 45–56 (1999).
33. B. Poddevin et al., "Very high cytotoxicity of bleomycin introduced into the cytosol of cells in culture," *Biochem. Pharmacol.* **42**(Suppl 1), S67–S75 (1991).
34. L. G. Salford et al., "A new brain tumor therapy combining bleomycin with in vivo electroporation," *Biochem. Biophys. Res. Commun.* **194**(2), 938–943 (1993).

Biographies for the authors are not available.